



**Short communication**

## Different pattern of changes in calcium binding proteins immunoreactivity in the medial prefrontal cortex of rats exposed to stress models of depression

Monika Zadrożna<sup>1</sup>, Barbara Nowak<sup>1</sup>, Magdalena Łasoń-Tyburkiewicz<sup>3</sup>,  
Małgorzata Wolak<sup>1</sup>, Magdalena Sowa-Kućma<sup>3</sup>, Mariusz Papp<sup>3</sup>,  
Grażyna Ossowska<sup>2</sup>, Andrzej Pilc<sup>3,4</sup>, Gabriel Nowak<sup>1,3</sup>

<sup>1</sup>Chair of Pharmacobiology, Jagiellonian University, Collegium Medicum, Medyczna 9, PL 30-688 Kraków, Poland

<sup>2</sup>Department of Pharmacology and Clinical Pharmacology, Medical University of Lublin, Jaczewskiego 8, PL 20-090 Lublin, Poland

<sup>3</sup>Institute of Pharmacology, Polish Academy of Sciences, Smętna 12, 31-343 PL Kraków, Poland

<sup>4</sup>Institute of Public Health, Jagiellonian University, Collegium Medicum, Grzegórzecka 20, PL 31-531 Kraków, Poland

**Correspondence:** Monika Zadrożna, e-mail: mfzadroz@cyf-kr.edu.pl

---

### Abstract:

Reductions in the number and size of neurons in the medial prefrontal cortex (mPFC) have been documented in many post-mortem studies of depressed patients and animals exposed to stress. Here, we examined the effect of chronic unpredictable stress (CUS) and chronic mild stress (CMS) on specific populations of neurons in the rat mPFC. Antibodies directed against parvalbumin (PV), calbindin D-28K (CB) and active caspase-3 have been used to quantify the numerical density of PV-immunoreactive (PV-ir), CB-ir and active caspase-3-ir cells, and to measure the relative optical density of neuropil. CUS decreased the density of CB-ir neurons and the optical density of CB-ir neuropil. In turn, CMS increased the densities of both CB-ir neurons and neuropil, while PV-ir neurons and PV-ir neuropil were not changed. The frequency distribution of neuronal surface areas was significantly different only for PV-ir neurons, and only between the control and CUS group. CMS reduced the density of active caspase-3-ir cells while CUS did not. We concluded that the mPFC reveals a different pattern of changes in neurons containing calcium binding proteins and active caspase-3 immunoreactivity in response to CUS and CMS.

### Key words:

CUS, CMS, mPFC, parvalbumin, calbindin D-28K, caspase-3, immunohistochemistry

---

**Abbreviations:** CB – calbindin D-28K, CB-ir – calbindin D-28K immunoreactive, CMS – chronic mild stress, CUS – chronic unpredictable stress, mPFC – medial prefrontal cortex, PV – parvalbumin, PV-ir – parvalbumin immunoreactive, ROD – relative optical density

### Introduction

Animal models of depression such as the chronic mild (CMS) or chronic unpredictable stress (CUS) have

proved to be valuable tools in understanding the neurobiological relationship between stress and depression [36]. The model of CUS is caused by treating the animals with different stress stimuli in an unpredictable sequence. The CMS is an experimental animal model of induced anhedony, created through the exposure of rats to a variety of very mild stressors [36]. Stress and depression are associated with abnormalities of the central nervous system [33]. It has been reported in experimental animals that chronic stress, can affect brain activity and induce localized structural changes and neuronal damage [18, 25]. Additionally, stress in animals evokes a loss of neurons that mimic neuronal changes observed in depressed patients [13]. A neuroanatomical region very sensitive to stress exposure is the prefrontal cortex (PFC) [5]. In rats, the medial PFC (mPFC) is suggested to share its analogous function with the PFC in humans and appears to be involved in the working of memory, attention and reward, which themselves are affected in several psychiatric disorders, such as schizophrenia or depression [26]. Postmortem studies of patients suffering from major depression have shown a decreased number and size of neurons and glia in the mPFC as well as a related decreased volume of the mPFC [29]. However, little is known about the effect of CUS and CMS on the density and size of interneurons in the rat mPFC.

In the present study, we investigated immunohistochemical changes in two neuronal populations with broad distributions containing calcium-binding proteins: parvalbumin (PV) and calbindin D-28K (CB) in the mPFC of the rats exposed to CUS and CMS. Both PV and CB are valuable anatomical markers and have been shown to exist independently within the subpopulation of GABAergic interneurons [11]. PV-immunoreactive (ir) and CB-ir interneurons are known to provide the inhibitory input to the perisomatic region of principal cells in many brain areas [32].

Recent studies also demonstrate that chronic stress/depression may also trigger apoptosis [23], so we therefore identified the apoptotic cells by assessing the active caspase-3 immunoreactivity. Caspase-3 is a member of the cysteine protease family, which plays a crucial role in apoptotic pathways by cleaving a variety of key cellular proteins. When stimuli activate caspase-3 in neurons and glial cells, the cells are committed to die [37]. Thus, activation of caspase-3 is essential in apoptosis.

## Materials and Methods

### Animals

Male Wistar rats (250–270 g) were used in the experiments. The animals were maintained in temperature and humidity-controlled rooms ( $22 \pm 2^\circ\text{C}$  and humidity:  $55 \pm 5\%$ ) with a light/dark cycle of 12 hours on, 12 hours off, and with free access to food and water. The experiments were carried out between 9:00 a.m. and 2 p.m. Each experimental group consisted of 8–12 animals. The control groups did not reveal differences in the morphological and immunohistochemical studies, so we have therefore presented only one of the groups. The procedures were conducted according to NIH Animal Care and Use Committee guidelines, and were approved by the Ethics Committee of the Medical University of Lublin and the Ethics Committee at the Institute of Pharmacology, Polish Academy of Sciences in Kraków.

### CUS and CMS procedures

The chronic unpredictable stress (CUS) procedure was a variant of the Katz method [17]; the CMS paradigm developed as a result of Willner's modification [36] – details of the methods used here have been published previously [27].

### Brain preparation

After decapitation, the brains were removed from the skull and the limbic forebrains (excluding the olfactory bulbs) were quickly sectioned and fixed in a neutral phosphate-buffered 4% formaldehyde solution. They were then dehydrated in a graded series of ethanol and embedded in paraffin. Fifteen-micrometer-thick paraffin sections were cut in the coronal plane and mounted on slides. To obtain the mPFC, tissue sections were collected through the following brain positions: from 3.70 mm to 2.20 mm from the bregma, according to the rat brain atlas of Paxinos and Watson [28].

### Immunohistochemistry (IHC)

IHC labeling was performed with the standard LAB-SA method (LAB-SA Detection System, ZYMED, USA). Paraffin sections were dewaxed and rehydrated ac-

cording to standard procedures. To retrieve antigen, slides were heated from 92 to 96°C in a 10 mM citrate buffer (pH = 6.0) for 20 min. Next, they were quenched sequentially in 1% H<sub>2</sub>O<sub>2</sub> in methanol for 30 min, blocked with normal serum (ZYMED Labs, USA) and incubated in a moist chamber at 4°C overnight with primary antibody (polyclonal anti-calbindin D-28K, Chemicon, 1:750; monoclonal anti-parvalbumin, Sigma-Aldrich, 1:1000; polyclonal anti-active caspase-3, Chemicon, 1:10). After several washes in PBS, the sections were incubated with the appropriate biotinylated secondary antibodies (ZYMED Labs, USA) for 10 min at room temperature, and the streptavidin-peroxidase complex (ZYMED Labs, USA) for 10 min at room temperature. The binding of primary antibody was visualized using diaminobenzidine (Invitrogen Ltd., UK) for 8 min. After washing with distilled water, some sections were counterstained with a Nissl substance, dehydrated in ethanol and xylene and mounted in the DPX medium (Fluka).

IHC controls: No labeling was detected when primary antibodies were omitted.

### Quantitative evaluation

All counts were performed at 40× and 100× (objective lens) under a light microscope (Olympus BX41, Japan) plus a microcomputer microscope image analyzer combined with the Imaging Software Cell-D.

The mPFC consists of three subregions (anterior cingulate, prelimbic and infralimbic cortices) and we merged these three areas and presented the pooled data for the mPFC. An average of 6 sections (200 μm apart) per every type of immunoreaction, taken from each animal, were analyzed. The immunoreactive neurons were counted in five randomly selected columns going perpendicularly from the pial surface to the white matter along the whole cortical depth. The width of the cortical column was 104 μm and its total height corresponded to the cortical depth. In each column, the non-overlapping contiguous counting images of 104 μm width and 138 μm high (100× objective) were made. The data were presented as the mean numerical density per 0.1 square millimeter of the cortical column. The immunostained neuronal density (P) per unit area was estimated using the Abercrombie formula:  $P = A \times M / L + M$  [1], where M = section thickness in microns (15 μm); L = mean nuclear diameter of the respective area; A = crude neuronal

count per 0.1 sq. mm. In addition, the relative optical density (ROD) of the immunoreactive neuropil excluding the cell bodies was measured in each image and for both CB and PV immunostaining. The optical density (OD) of the area of interest was related to the background value by the formula:  $[\text{OD area} - \text{OD background}] / \text{OD background} \times 100$ , thus eliminating the variability in background staining among sections [21]. Also, the mean area of the CB-ir and PV-ir neuronal pericaryon was measured by means of our specifically designed software only if the nucleus of the marked neuron was visible. We measured about 100 labeled neurons per case. Neuronal areas are presented as frequency histograms by size class.

### Data analysis and statistics.

Results are expressed as the group means ± SEM. Comparisons between the groups were carried out using Kruskal-Wallis one-way analysis of variance and Dunn's multiple comparison *post-hoc* test. To assess the correlation values between the selected parameters the Pearson correlation was used. The level of statistical significance was set at  $p < 0.05$ .

## Results

### Calcium-binding proteins

The observation of immunoreactive neurons indicates that PV-ir neurons were present throughout the layers II-VI of the mPFC in both CUS and CMS rats, whereas CB-ir neuronal cell bodies with moderate to intense immunoreactivity were located in all layers but mostly in layers II + III (Fig. 1). We also observed pericellular clusters of PV-ir puncta surrounding unlabelled cellular profiles (Fig. 2D).

The majority of cell types containing the PV and CB are interneurons; however, some pyramidal cells might also contain these proteins. In the present study we observed a low intensity of PV and CB labelled pyramidal cells (Fig. 2B), but they were not included for analysis.

No significant differences in the mean numerical density of PV-ir neurons were observed between stressed groups and the control group (Fig. 1A). On the other hand, there were significant differences be-

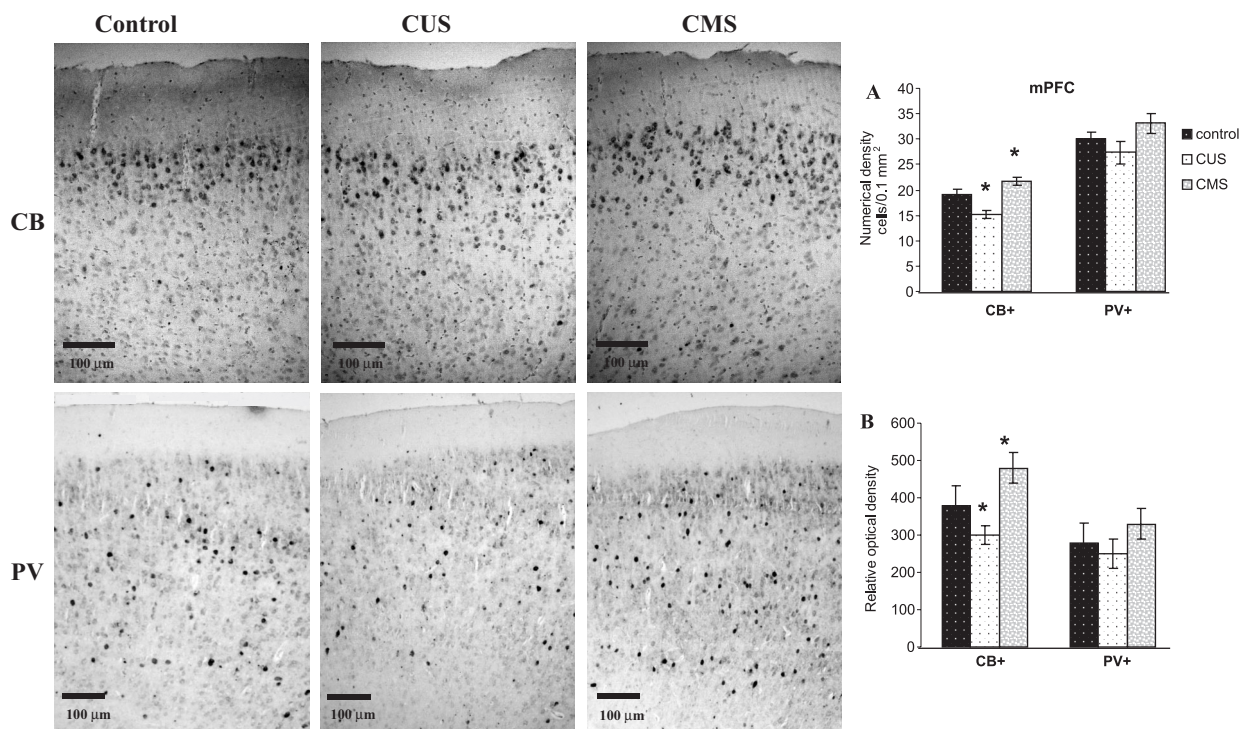


**Fig. 1.** Impact of chronic stress on CB and PV immunoreactivity in the rat mPFC. Left panel – Distribution of CB- and PV-ir neurons in the mPFC. Right panel – **(A)** Numerical density  $\pm$  SEM of CB and PV-positive cells per 0.1 mm<sup>2</sup> in the mPFC of studied groups. **(B)** Relative optical density  $\pm$  SEM of CB and PV in the rat mPFC of stressed and control animals. \*  $p < 0.05$  compared with the control group (ANOVA Kruskal-Wallis and Dunn *post-hoc* test)

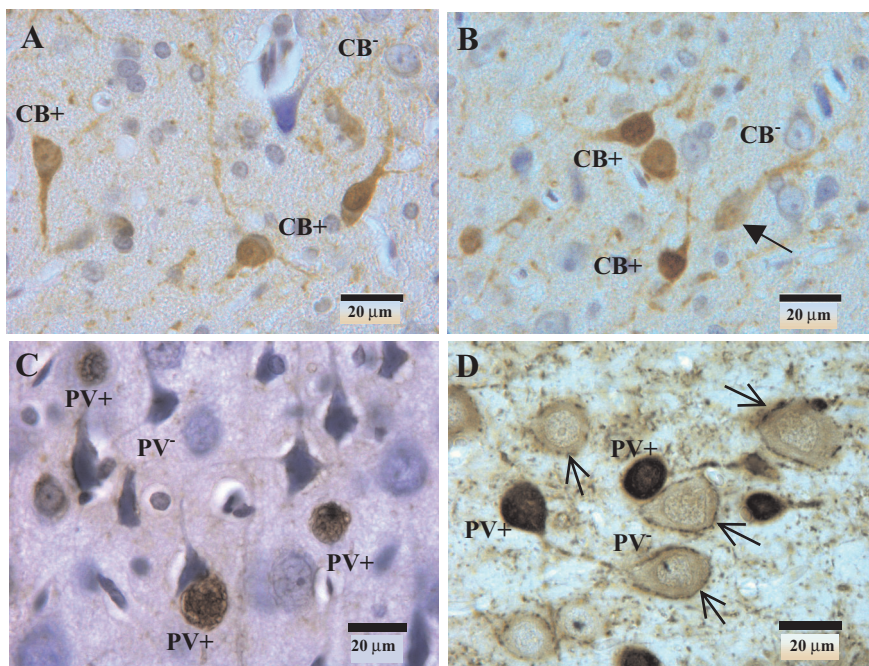
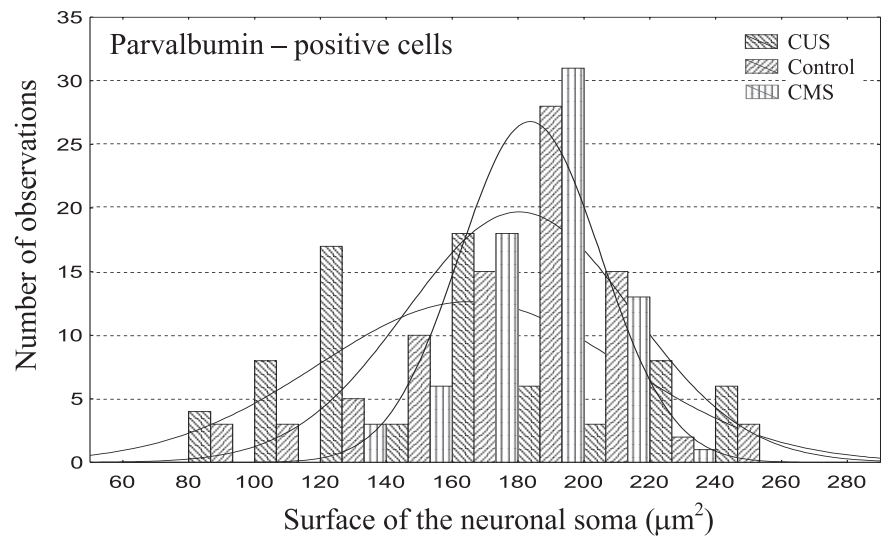


**Fig. 2.** High-power photomicrographs illustrating calbindin-D28K-positive cells (CB+) and negative cells (CB-) and parvalbumin-positive cells (PV+) and negative cells (PV-) in the lower layer of the mPFC of the studied materials. **(A)** and **(B)** showing CB immunohistochemical reaction and Nissl counterstaining, thick arrow – the somatic profile of the pyramidal neuron displaying weak CB immunoreactivity. **(C)** PV immunoreactivity and Nissl staining. **(D)** showing only PV immunostaining, thin arrows – PV+ puncta forming complete pericellular clusters around the somata of unlabelled neurons

**Fig. 3.** Distribution of the areas of PV-ir neuronal profiles in the mPFC of CUS, CMS and control groups



tween the CUS and the control, and the CMS and control group in the mean density of CB-ir neurons. We observed a reduction by 20% in the CUS group ( $H = 7.13$ ;  $p < 0.05$ ) and an increase by 14% in the CMS group when compared to the control group ( $H = 6.11$ ;  $p < 0.05$ ; Fig. 1A). The ROD of the neuropil showed significant differences only in the CB-ir material (Fig. 1B) and correlated with the numerical density of CB-ir neurons in CUS ( $r = 0.3728$ ;  $p < 0.05$ ) and CMS group ( $r = 0.3531$ ;  $p < 0.05$ ).

The frequency distribution of neuronal surface areas was significantly different ( $H = 4.98$ ;  $p < 0.05$ ) only for PV-ir neurons, and only between the control and CUS groups. Indeed, in the mPFC, there are more

small PV-ir neuronal profiles in CUS cases (in the frequency class 80–140  $\mu\text{m}^2$ ) and markedly less large profiles in the frequency class 180–220  $\mu\text{m}^2$  (Fig. 3).

### Cell apoptosis

To identify apoptotic cells in tissue sections we used active caspase-3 immunoreactivity and Nissl staining. Caspase-3-ir cells were mostly localized in deeper layers of the mPFC. They usually did not display well-developed morphological signs of apoptosis, consistent with the fact that caspase-3 activation is an early phenomenon preceding DNA strand breakage and terminal nuclear and cytoplasmic changes [30].

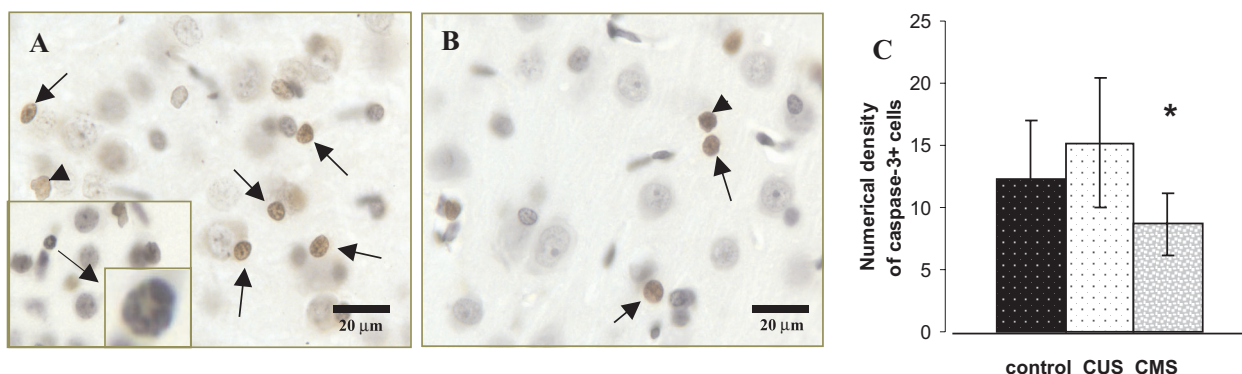


**Fig. 4.** Impact of chronic stress on the number of active caspase-3-positive cells in the mPFC. (A) and (B) Examples of active caspase-3-ir cells in CUS and CMS groups, respectively. Arrows indicate active caspase-3-positive cells, arrow heads – shrunken cells. The boxed regions show apoptotic bodies, a morphologic hallmark of apoptosis. Sections were counterstained with a Nissl substance. (C) Results are expressed as the mean  $\pm$  SEM numerical density of active caspase-3-positive cells. \*  $p < 0.05$  compared with the control group (ANOVA Kruskal-Wallis and Dunn *post-hoc* test)

---

However, little multiple apoptotic bodies were observed (Fig. 4), especially in CUS material. The presence of apoptotic body formation was not accompanied by active caspase-3 immunoreactivity. Caspase-3-ir cells were round in shape and similar to or somewhat smaller than Nissl-stained small neurons. Caspase-3 immunoreactivity was also seen in small shrunken cells (Fig. 4). CMS decreased the numerical density of active caspase-3-ir cells in comparison to the control material ( $H = 5.41$ ;  $p < 0.05$ ), but no differences in the density of active caspase-3-ir cells were observed in the CUS and control groups (Fig. 4).

---

## Discussion

The different influence of two animal models of depression, CUS and CMS, on studied calcium-binding proteins' immunoreactivity in the rat mPFC was determined in this study. A statistically significant decrease in the density of CB-ir neurons in the mPFC was caused by CUS. On the other hand, in animals exposed to CMS a significant increase in the density of CB-ir neurons was observed. Analogically to the numerical density of CB-ir neurons in the mPFC, the ROD of CB-ir neuropil was adequately lower in CUS but higher in CMS subjected rats. Both the numerical density of PV-ir neurons and the OD of PV-ir neuropil revealed a statistically non-significant tendency for a reduction in CUS mPFC and a tendency for an increase in CMS rats.

Previous studies did not show consistent results concerning the densities of PV and CB neurons in the PFC of the various human diseases. Both the increase [10] and decrease [2] of CB-ir neurons or no change in the density of these neurons [34] were observed in, for example, PFC of schizophrenic patients. Satoh et al. [31], observed a decrease of the number and size of PV-ir neurons in the PFC of models with Alzheimer's disease. On the other hand, Hof and Morrison [15] did not find changes in the density of these neurons in this disease. Almost a 50% decrease of density of CB-ir neurons in II + III layers of the dorsolateral PFC was described in major depressive disorder, whereas no significant changes were observed in the number of PV-ir neurons [29]. The decrease of neurons was also observed in animal models of stress [13], therefore, the demonstration of the increase of the density of CB neurons in the mPFC of rats that were exposed to

CMS is puzzling. Although it is admitted that the neurogenesis is limited to such places as the hippocampus or olfactory bulbs in the adult brain, Dayer et al. [9] and Gould et al. [12] also found the neurogenesis in the PFC of adult rats and nonhuman primates, although these results were questioned by other researchers [20]. Other studies showed that most newly developed cells in the mPFC demonstrate the expression of the neuron-glia 2 (NG2) [8, 24] marker in the population of glial cells. These glial cells can differentiate in GABAergic neurons [3, 9]. Besides, it is possible that the difference found in the density of CB-ir cells does not only depend on a reduction or increase of cell number but on the decrease or increase of protein expression.

Some significant differences regarding the distribution of PV-ir neuronal perikarya between the CUS and control groups were found in our study, suggesting changes in the sizes of the neuronal body. The changes in the size and the absence of significant differences in the numerical density of PV-ir neurons between the CUS and control groups could indicate a shift from large toward smaller areas for neuronal perikarya. It is well documented that stress results in glutamatergic neurotransmission in the PFC [22]. Excessive glutamate release can lead to excitotoxicity, thus neurons need to protect themselves by reducing their surface area. This reduction will diminish the amount of synaptic input [22], indicating alterations in neurotransmission. Moreover, interneurons demonstrating an expression of parvalbumin produce short-lived, fast-spiking action potential (FS) [11] and shows little or no adaptation when compared with regular spiking (RS) neurons [7]. RS interneurons demonstrate an expression of calbindin [11].

Hugon et al. [16] reported that CB-containing neurons exposed to oxidative stress in the cerebral cortex survive more often than neurons without CB. In our study, the increase of the density of CB-ir neurons and CB-ir of neuropil in the CMS group was accompanied by a decrease of cells demonstrating an expression of active caspase-3, whose activation is essential in neuronal apoptosis [37]. These results might suggest that CB could participate in neuroprotection after exposure to different mild stressors. This is in accordance with evidence showing that CB has a major role in different cell types in the protection against apoptotic cell death [6], and biochemical evidence showing that in osteoblasts, CB binds directly to caspase-3 and inhibits its activity [4].

In our study, caspase-3 positive cells were similar to or somewhat smaller than Nissl-stained small neurons and they did not usually display well-developed morphological signs of apoptosis. However, apoptotic body formation without active caspase-3 immunoreactivity was observed, especially in the CUS material. These observations may indicate different patterns of cellular death, which is a classical apoptosis with the expression of active caspase-3 or caspase-independent apoptosis often mediated by other proteases [35]. On the other hand, recent evidence has suggested that caspase-3 can be also involved in cellular processes such as neuronal differentiation, migration and plasticity [14], in addition to its role in cell death, and has shown that it is localized both in neurons and in glial cells [19]. Therefore, further studies of the apoptotic cell death markers, for example DNA fragmentation, are required as well as double immunostaining for caspase-3 and interneurons.

## Conclusion

The obtained results show that the mPFC reveals a different pattern of changes in calcium binding proteins and active caspase-3 immunoreactivity in response to CUS and CMS. CUS as an animal model of depression can be related to the decrease density of neurons containing CB in the mPFC. Opposite to this, however, the CMS demonstrated an increase of CB-containing neurons with a significant decrease of caspase-3-positive cells in the rat mPFC when compared with the control material. Further investigations are required.

## References:

1. Abercrombie M: Estimation of nuclear population from microtome sections. *Anat Rec*, 1946, 94, 239–247.
2. Beasley CL, Zhang ZJ, Patten I, Reynolds GP: Selective deficits in prefrontal cortical GABAergic neurons in schizophrenia defined by the presence of calcium-binding proteins. *Biol Psychiatry*, 2002, 52, 708–715.
3. Belachew S, Chittajallu R, Aguirre AA, Yuan X, Kirby M, Anderson S, Gallo V: Postnatal NG2 proteoglycan-expressing progenitor cells are intrinsically multipotent and generate functional neurons. *J Cell Biol*, 2003, 161, 169–86.
4. Bellido T, Huening M, Raval-Pandya M, Manolagas SC, Christakos S: Calbindin-D28k is expressed in osteoblastic cells and suppresses their apoptosis by inhibiting caspase-3 activity. *J Biol Chem*, 2000, 275, 26328–26332.
5. Cerqueira JJ, Mailliet F, Almeida OF, Jay TM, Sousa N: The prefrontal cortex as a key target of the maladaptive response to stress. *J Neurosci*, 2007, 27, 2781–2787.
6. Christakos S, Liu Y: Biological action and mechanism of action of calbindin in the process of apoptosis. *J Steroid Biochem Mol Biol*, 2004, 89–90, 401–404.
7. Connors BW, Gutnick MJ: Intrinsic firing patterns of diverse neocortical neurons. *Trends Neurosci*, 1990, 13, 99–104.
8. Czeh B, Muller-Keuker JI, Rygula R, Abumaria N, Hiemke C, Domenici E, Fuchs E: Chronic social stress inhibits cell proliferation in the adult medial prefrontal cortex: hemispheric asymmetry and reversal by fluoxetine treatment. *Neuropsychopharmacology*, 2007, 32, 1490–503.
9. Dayer AG, Cleaver KM, Abouantoun T, Cameron HA: New GABAergic interneurons in the adult neocortex and striatum are generated from different precursors. *J Cell Biol*, 2005, 168, 415–27.
10. Daviss SR, Lewis DA: Local circuit neurons of the prefrontal cortex in schizophrenia: selective increase in the density of calbindin-immunoreactive neurons. *Psychiatry Res*, 1995, 59, 81–96.
11. DeFelipe J: Types of neurons, synaptic connections and chemical characteristics of cells immunoreactive for calbindin-D28K, parvalbumin and calretinin in the neocortex. *J Chem Neuroanat*, 1997, 14, 1–19.
12. Gould E, Reeves AJ, Graziano MS, Gross CG: Neurogenesis in the neocortex of adult primates. *Science*, 1999, 286, 548–52.
13. Gould E, Tanapat P: Stress and hippocampal neurogenesis. *Biol Psychiatry*, 1999, 46, 1472–1479.
14. Gulyaeva NV: Non-apoptotic functions of caspase in the nervous system. *Biokhimiya*, 2003, 68, 1459–1470.
15. Hof PR, Morrison JH: Neocortical neuronal subpopulations labeled by a monoclonal antibody to calbindin exhibit differential vulnerability in Alzheimer's disease. *Exp Neurol*, 1991, 111, 293–301.
16. Hugon J, Hugon F, Esclaire F, Lesort M, Diop AG: The presence of calbindin in rat cortical neurons protects in vitro from oxidative stress. *Brain Res*, 1996, 707, 288–292.
17. Katz RJ, Roth KA, Carroll BJ: Acute and chronic stress affects open field activity in the rat: implication for a model of depression. *Neurosci Biobehav Rev*, 1981, 5, 247–251.
18. Kaufman J, Plotsky PM, Nemeroff CB, Charney DS: Effects of early adverse experiences on brain structure and function: clinical implications. *Biol Psychiatry*, 2000, 48, 778–790.
19. Kitamura Y, Taniguchi T, Shimohama S: Apoptotic cell death in neurons and glial cells: Implications for Alzheimer's Disease. *Jpn J Pharmacol*, 1999, 79, 1–5.
20. Kornack DR, Rakic P: Cell proliferation without neurogenesis in adult primate neocortex. *Science*, 2001, 294, 2127–2130.

- 
21. Krugers HJ, Koolhaas JM, Medema RM, Korf J: Prolonged subordination stress increases Calbindin-D28k immunoreactivity in the rat hippocampal CA1 area. *Brain Res*, 1996, 729, 289–293.
  22. Liu RJ, Aghajanian GK: Stress blunts serotonin-hypocretin-evoked EPSCs in prefrontal cortex: role of corticosterone-mediated apical dendritic atrophy. *Proc Natl Acad Sci USA*, 2008, 105, 359–364.
  23. Lucassen PJ, Vollmann-Honsdorf GK, Gleisberg M, Czech B, De Kloet ER, Fuchs E: Chronic psychosocial stress differentially affects apoptosis in hippocampal subregions and cortex of the adult tree shrew. *Eur J Neurosci*, 2001, 14, 161–166.
  24. Madsen TM, Yeh DD, Valentine GW, Duman RS: Electroconvulsive seizure treatment increases cell proliferation in rat frontal cortex. *Neuropsychopharmacology*, 2005, 30, 27–34.
  25. McEwen BS: Effects of adverse experiences for brain structure and function. *Biol Psychiatry*, 2000, 48, 721–731.
  26. Miller EK, Cohen JD: An integrative theory of prefrontal cortex function. *Annu Rev Neurosci*, 2001, 24, 167–202.
  27. Nowak B, Zadrożna M, Ossowska G, Sowa-Kućma M, Gruca P, Papp M, Dybała M et al.: Alterations in hippocampal calcium binding neurons induced by stress models of depression. Preliminary assessment. *Pharmacol Rep*, 2010, 62, 1204–1210.
  28. Paxinos G, Watson GC: *The Rat Brain*, 4th edn. Academic Press, San Diego, 1998.
  29. Rajkowska G, O'Dwyer G, Teleki Z, Stockmeier CA, Miguel-Hidalgo J: GABAergic neurons immunoreactive for calcium binding proteins are reduced in the prefrontal cortex in major depression. *Neuropsychopharmacology*, 2007, 32, 471–482.
  30. Sakahira H, Enari M, Nagata S: Cleavage of cad inhibitor in cad activation and DNA degradation during apoptosis. *Nature*, 1998, 391, 96–99.
  31. Satoh J, Tabira T, Sano M, Nakayama H, Tateishi J: Parvalbumin-immunoreactive neurons in the human central nervous system are decreased in Alzheimer's disease. *Acta Neuropathol*, 1991, 81, 388–395.
  32. Seress L, Leranth C, Frotscher M: Distribution of calbindin D28k immunoreactive cells and fibers in the monkey hippocampus, subicular complex and entorhinal cortex. A light and electron microscopic study. *J Hirnforsch*, 1994, 35, 473–86.
  33. Szymańska M, Suska A, Budziszewska B, Jaworska-Feil L, Basta-Kaim A, Leśkiewicz M, Kubera M et al.: Prenatal stress decreases glycogen synthase kinase-3 phosphorylation in the rat frontal cortex. *Pharmacol Rep*, 2009, 61, 612–620.
  34. Tooney PA, Chahl LA: Neurons expressing calcium-binding proteins in the prefrontal cortex in schizophrenia. *Prog Neuropsychopharmacol Biol Psychiatry*, 2004, 28, 273–278.
  35. Volbracht C, Leist M, Kolb SA, Nicotera P: Apoptosis in caspase-inhibited neurons. *Mol Med*, 2001, 7, 36–48.
  36. Willner P: Chronic mild stress (CMS) revisited: Consistency and behavioural-neurobiological concordance in the effects of CMS. *Neuropsychobiology*, 2005, 52, 90–110.
  37. Yuan J, Yankner BA: Apoptosis in the nervous system. *Nature*, 2000, 407, 802–809.

**Received:** November 3, 2010; **in the revised form:** June 17, 2011; **accepted:** June 28, 2011.